Real-time gait planning for Rh-1 humanoid robot, using Local Axis Gait algorithm

Conference Paper *in* International Journal of Humanoid Robotics · January 2008

DOI: 10.1109/ICHR.2007.4813927 · Source: IEEE Xplore

CITATIONS
14

READS
71

2 authors, including:

M. Arbulu
National Open University and Distance (Colombia)
49 PUBLICATIONS **111** CITATIONS

SEE PROFILE

Real-Time gait planning for Rh-1 humanoid robot, using Local Axis Gait algorithm

Mario Arbulu, Carlos Balaguer

Robotics Lab, Department of System and Automation Engineering, University Carlos III of Madrid
Av. de la Universidad 30, 28911, Legans, Madrid, Spain
marbulu@ing.uc3m.es
balaguer@ing.uc3m.es

***Abstract*— It is proposed the Local Axis Gait algorithm in order to generate real-time gait patterns for a humanoid robot. The 3D foot motion planning for the humanoid global motion is developed in order to walk in any surface as plane, ramp, climbing stairs. Furthermore, it is possible continuous change the step length and orientation in real time. The cart-table model is used for planning COG and ZMP motion. The proposed algorithm takes into account physical robot constraints as joint angles, angular velocity and torques. Torques are computed by Lagrange method under Lie groups. Some results are shown and discussed.**

I. Introduction

Several works about gait pattern generation have been developed. It is well known that the humanoid motion planning uses COG and swing foot motion as reference patterns. The COG motion maintain the robot stability and the swing foot motion allows the humanoid change its global position, so it is necessary to develop suitable trajectories for each humanoid robot step. Mass distributed model developed i.e. Takanishi et. al [1], Vukobratovic et. al [2], taking into account each mass link in order to compute the ZMP by a complex dynamic model. The well known mass concentrated model i.e Kajita et. al. [3], [4], simplify the complex and non-linear humanoid robot dynamics to linear one, by concentrating the overall robot mass in its COG (center of gravity) and constraining the motion to any arbitrary plane. So, it is possible to develop the COG motion by following the inverted pendulum laws, in this paper it is used. Nevertheless, the foot motion planning is not clearly explained in any works [5], [6]. For that, in this paper this fact will be detailed. Foot motion planning should taken into account allowing the angular joint, angular velocity and torque constraints, in specially the knee joint; furthermore, avoiding collisions with support leg (internal collisions) and with any obstacle on walking surface (external collisions). It is obtained continuous walking motion while changing direction, as human natural walking. The present work is divided as following: at first, in section II, foot motion planning is developed. In section III, COG and ZMP motion planning is explained. In the section IV, Lagrange formulation using Lie groups and Screw theory is developed in order to verify the joints torque constraints. In section V, some simulation on Rh- 1 simulator and experimental results on Rh-1 humanoid platform are shown and discussed. Finally in section VI the conclusions of this work are presented.

II. Foot Motion Planning

A. Overview

In order to change the global position of the humanoid robot, the swing foot should change its configuration from initial position and orientation to goal position and orientation. The goal configuration is limited by the physical constraint of the robot as, angular joint limits, angular joint velocities, angular accelerations, singularities and joint torques. The kinematics model using lie groups, which $\in$ SE(3) [7], [8], allows to avoid internal singularities, so the problem is to avoid the external ones. The dynamics model use the Lagrange formulation and lie groups, and it is possible to compute the joint torques accurately (eq. 1 and 2).

$$L\left(\theta,\dot{\theta}\right) = K\left(\theta,\dot{\theta}\right) - V\left(\theta\right), \tag{1}$$

K models the potential energy effect over the body and V models the kinetics energy over one. So the motion equation is the following 2:

$$\frac{d}{dt}\left(\frac{\partial L}{\partial \dot{\theta}}\right) - \frac{\partial L}{\partial \theta} = \Gamma, \tag{2}$$

Where Γ, is the torque due to the inertial force and gravity field and it will be detailed, in the next sections. The 3D foot motion planning for carrying out the n^{th} step can be modeled, as shown in Fig. 1. The swing foot moves from initial configuration (position and orientation $(n-1)^{th}$ frame) to the goal configuration (position and orientation $(n+1)^{th}$ frame). The input parameters are the swing foot goal configuration (position and orientation), defined in the appropriate local axis as: $(L_x, L_y, L_z, \theta_x, \theta_y, \theta_z)^{n+1}$. It is possible to identify the parameters and frames for the n^{th} step as follows:

$\sum$: World frame
$\sum^n$: n^{th} local configuration frame, support foot
$\sum^{n-1}$: $(n-1)^{th}$ local configuration frame, swing foot
$\sum^{n+1}$: $(n+1)^{th}$ local configuration frame, swing foot
p^n : n^{th} position of support foot local frame
p^{n-1} : $(n-1)^{th}$ position of swing foot local frame
p^{n+1} : $(n+1)^{th}$ position of swing foot local frame
L_x^{n+1}: $(n+1)^{th}$ frontal swing foot motion (x)
L_y^{n+1}: $(n+1)^{th}$ lateral swing foot motion (y)

L_z^{n+1}: $(n+1)^{th}$ vertical swing foot motion (z)
θ_x^{n+1}: $(n+1)^{th}$ rotation in X axis world
θ_y^{n+1}: $(n+1)^{th}$ rotation in Y axis world
θ_z^{n+1}: $(n+1)^{th}$ rotation in Z axis world

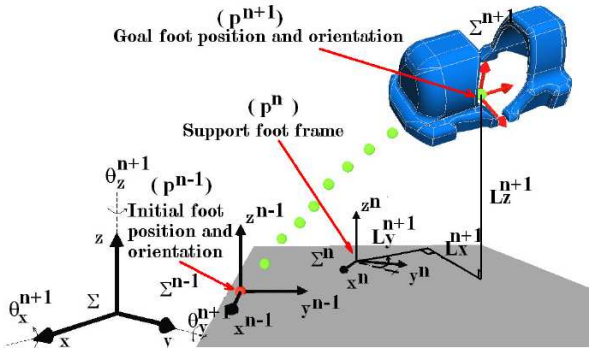

Fig. 1. Swing foot (SF) and reference frames for 3D planning motion on each step. In this case, the n^{th} step planning is shown.

B. Motion Interpolators

Polynomials have been used for approximation because they can be evaluated, differentiated, and integrated easily and infinitely for many steps using just basic arithmetic operations of addition, subtraction and multiplication. A polynomial of order n or degree n is a function of the form:

$$\phi(t) = w_1 + w_2.t + ... + w_n.t^{n-1} = \sum_{k=1}^{n} w_k.t^{k-1} \quad (3)$$

Where $\phi(t) \in Q^n$, with Q^n being the set or linear space of all polynomials (eq. 3) of order n . The swing foot (SF) motion is planned by two fifth order interpolators (eq. 4) one for climbing the foot ($\phi_1(t)$, eq. 4) and one for landing the foot ($\phi_2(t)$, eq. 4), on each axis motion and orientation motion. These allow us to control the foot position, velocity and acceleration, so is minimized the foot landing reacting force and the knee angular velocity and smooth and natural joints motion are obtained.

$$\phi(t) = \begin{cases} \phi_1\left(t, x_i^1, \dot{x}_i^1, \ddot{x}_i^1, x_f^1, \dot{x}_f^1, \ddot{x}_f^1\right) \quad \forall \quad 0 \le t < \frac{T}{2} \\ \quad \phi_1(t) = w_6^1.t^5 + w_5^1.t^4 + w_4^1.t^3 + w_3^1.t^2 ... \\ \quad +w_2^1.t + w_1^1 \\ \\ \phi_2\left(t, x_i^2, \dot{x}_i^2, \ddot{x}_i^2, x_f^2, \dot{x}_f^2, \ddot{x}_f^2\right) \quad \forall \quad \frac{T}{2} \le t \le T \\ \quad \phi_2(t) = w_6^2.t^5 + w_5^2.t^4 + w_4^2.t^3 + w_3^2.t^2 ... \\ \quad +w_2^2.t + w_1^2 \end{cases} \quad (4)$$

Where the fifth order polynomial are characterized by the next boundary conditions on each zone; i.e. for *j-th* zone (*j*=1 for climbing, *j*=2 for landing):

T : Step time
x_i^j : Initial position, of *j-th* zone
$\dot{x}_i^j$: Initial velocity, of *j-th* zone
$\ddot{x}_i^j$: Initial acceleration, of *j-th* zone
x_f^j : Final position, of *j-th* zone
$\dot{x}_f^j$: Final velocity, of *j-th* zone
$\ddot{x}_f^j$: Final acceleration, of *j-th* zone

Hence the polynomial coefficients (eq. 5 to 10), can be developed as following from the boundary conditions described above:

$$w_1^j = x_i^j \quad (5)$$

$$w_2^j = \dot{x}_i^j \quad (6)$$

$$w_3^j = \frac{\ddot{x}_i^j}{2} \quad (7)$$

$$w_4^j = 10\left(\frac{x_f^j - x_i^j}{T^3} - \frac{\dot{x}_i^j}{T^2} - \frac{\ddot{x}_i^j}{2T}\right) - 4\left(\frac{\dot{x}_f^j - \dot{x}_i^j}{T^2} - \frac{\ddot{x}_i^j}{T}\right) + \\ .....\frac{1}{2}\left(\frac{\ddot{x}_f^j - \ddot{x}_i^j}{T}\right) \quad (8)$$

$$w_5^j = -15\left(\frac{x_f^j - x_i^j}{T^4} - \frac{\dot{x}_i^j}{T^3} - \frac{\ddot{x}_i^j}{2T^2}\right) + 7\left(\frac{\dot{x}_f^j - \dot{x}_i^j}{T^3} - \frac{\ddot{x}_i^j}{T^2}\right) - \\ .....\left(\frac{\ddot{x}_f^j - \ddot{x}_i^j}{T^2}\right) \quad (9)$$

$$w_6^j = 6\left(\frac{x_f^j - x_i^j}{T^5} - \frac{\dot{x}_i^j}{T^4} - \frac{\ddot{x}_i^j}{T^3}\right) - 3\left(\frac{\dot{x}_f^j - \dot{x}_i^j}{T^4} - \frac{\ddot{x}_i^j}{T^3}\right) + \\ .....\frac{1}{2}\left(\frac{\ddot{x}_f^j - \ddot{x}_i^j}{T^3}\right) \quad (10)$$

The continuity at the end of the climbing zone and at the start of the landing one should satisfy the following conditions:

$$\phi_1(T/2) = \phi_2(T/2) \quad (11)$$

$$\dot{\phi}_1(T/2) = \dot{\phi}_2(T/2) \quad (12)$$

$$\ddot{\phi}_1(T/2) = \ddot{\phi}_2(T/2) \quad (13)$$

C. Planning foot position and orientation

Goal foot configuration (position, P^{n+1}, and orientation, θ^{n+1}) are the input parameters for carrying out the next step. It can be done by humanoid sensors or external command. Those input parameters can be generalized in order to compute the n^{th} step in real time as:

$$P^n = P^{n-1} + R(\theta_z^n)^T.L^n \quad (14)$$

Where,

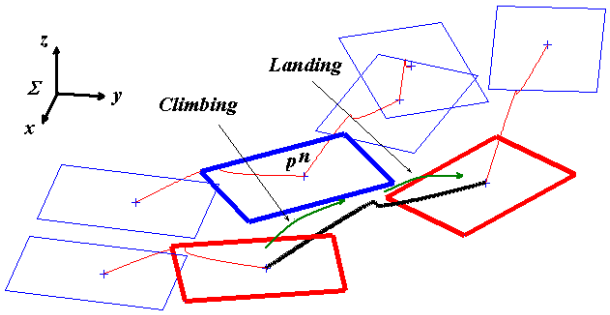

Fig. 2. Swing foot (SF) motion planning changing walking direction in real time. The *n-th* step trajectory is in black bold line, and the swing foot is represented by the red bold rectangles, while the support foot is represented by the blue bold rectangle.

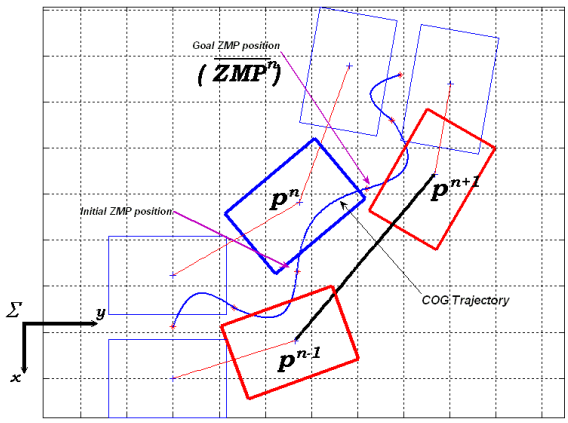

Fig. 3. ZMP and COG motion planning in the ***n-th*** step.

$$P^n = \begin{pmatrix} p_x^n \\ p_y^n \\ p_z^n \end{pmatrix},\ P^{n-1} = \begin{pmatrix} p_x^{n-1} \\ p_y^{n-1} \\ p_z^{n-1} \end{pmatrix},$$

$$R(\theta_z^n)^T = \begin{pmatrix} cos(\theta_z^n) & -sin(\theta_z^n) & 0 \\ sin(\theta_z^n) & cos(\theta_z^n) & 0 \\ 0 & 0 & 1 \end{pmatrix},\ L^n = \begin{pmatrix} L_x^n \\ \text{-(-1)}^n \text{L}_y^n \\ L_z^n \end{pmatrix}$$

As we see in eq. 14, the goal foot configuration depends on the support foot position, because the support foot is the local axis of gait input parameters. By applying in the splines developed above, between local axis *n-1-th* to *n+1-th* (from *n-1* swing foot configuration to *n+1* one) smooth and natural foot motion is obtained. Some simulation results are shown in Fig. 2. It is possible to walk changing direction and step length in real time by using the proposed algorithm. Any configuration motion can be obtained, but it is limited by the physical humanoid constraints such as angular joint motion, angular velocities and joint torques. The Lagrange method and screws are used to compute dynamic joint effects such as constraint torques. Furthermore, stability margin should be taken into account, so the ZMP must be maintained in the convex hull. The next section deals with stability humanoid robot motion.

III. COG AND ZMP MOTION PLANNING

At the ***n-th*** step, the ZMP reference must be in the P^n point in single support and between P^n and P^{n+1} in double support. Thus, we define two change foot points, at starting ***n-th*** step and at finishing one. These points will be defined as median ZMP ($\overline{ZMP}^n$).

It is possible to generalize the $\overline{ZMP}^n$ configuration as following (i.e. Fig. 3):

$$\overline{ZMP}^n = R(\theta_z^{n+1})^T.(L/2)^{n+1} \tag{15}$$

In order to define the ZMP and COG reference trajectories, the cart-table model (Kajita et. al., [3]) has been used. The control of the cart-table by the preview controler (i.e. Fig. 4), allows that the ZMP trajectory to be computed by the following equations:

$$ZMP_x = x - \frac{Z_c}{g}\ddot{x} \tag{16}$$

$$ZMP_y = y - \frac{Z_c}{g}\ddot{y} \tag{17}$$

Where ***x*** and ***y*** give us the **COG** trajectory (i.e. Fig. 3) at Z_c plane. Hence, given the reference **ZMP** trajectory, the **COG** one is an inverse problem.

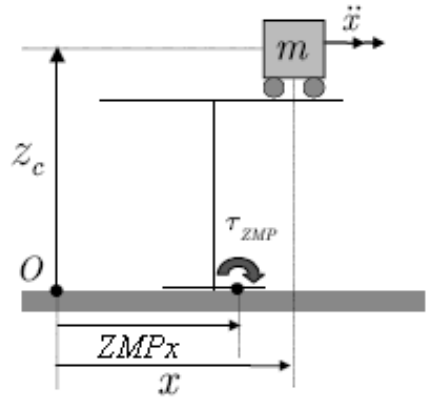

Fig. 4. A Cart-table model, on x-axis.

IV. DYNAMIC MODEL

A. Lagrange formulation (Lagrangian)

In order to compute the joint torques and dynamics constraints, a dynamic model should be proposed, so the Lagrange formulation under the lie groups and screw theory has been developed, because it gives us a natural description of Jacobian manipulator. The Lagrange formulation could be expressed as the following:

$$L\left(\theta,\dot{\theta}\right) = K\left(\theta,\dot{\theta}\right) - V\left(\theta\right) \tag{18}$$

Where $K(\theta,\dot{\theta})$ is the overall links kinetics energy contribution and $V(\theta)$ the potential one:

$$K\left(\theta,\dot{\theta}\right) = \sum_{i=1}^{n} K_i\left(\theta,\dot{\theta}\right) = \frac{1}{2}\dot{\theta}^T Mm\left(\theta\right)\dot{\theta} \tag{19}$$

$$V\left(\theta\right) = \sum_{i=1}^{n} V_i\left(\theta\right) = \sum_{i=1}^{n} m_i g h_i\left(\theta\right) \tag{20}$$

With the motion equation by Γ torques being the following:

$$\frac{d}{dt}\left(\frac{\partial L}{\partial \dot{\theta}}\right) - \frac{\partial L}{\partial \theta} = \Gamma, \tag{21}$$

Which could be expressed as the following:

$$M.m\left(\theta\right).\ddot{\theta} + N\left(\theta,\dot{\theta}\right) = \Gamma \tag{22}$$

So, $M.m(\theta) \in \Re^{nxn}$ is the inertial manipulator matrix and it is defined by the operational Jacobian manipulator J_{sli} and the inertial generalized matrix M_i as:

$$M.m\left(\theta\right) = \sum_{i=1}^{n} J_{sli}^T\left(\theta\right).M_i.J_{sli}\left(\theta\right) \tag{23}$$

The humanoid robot platform Rh-1, developed in the Roboticslab of the University Carlos III of Madrid, which had been used in this work, to test this algorithm; has 21 degrees of freedom, for this $M.m(\theta) \in \Re^{21x21}$. The angular acceleration vector is defined by $\ddot{\theta}$, in which has each joint angular acceleration. Thus the joints torque without potential forces have been made by $M.m(\theta).\ddot{\theta}$. The $N\left(\theta,\dot{\theta}\right)$ term gives us the joints torque due to the potential forces, and is defined as (eq. 24):

$$N\left(\theta,\dot{\theta}\right) = \frac{\partial V}{\partial \theta} \tag{24}$$

From (20) , $V\left(\theta\right) = \sum_{i=1}^{n} m_i g h_i\left(\theta\right)$, where m_i is the mass of the *i-th* link, *g* is the gravity acceleration and $h_i(\theta)$ the COG height of the *i-th* link.

B. Torque analysis

The joints torque for the n-th step lead us to compare with each joint actuator physical limit which is a dynamic constraint of gait pattern. Some results are shown in Fig. 5. The support foot joints from 8 to 12, the joint 7 is for horizontal motion and it is not shown. Two joints drive the frontal support leg motion: 8 (hip) and 12 (ankle). The next three joints drive the sagital support leg motion 9 (hip), 10 (knee), 11 (ankle). The joints actuator torque limits are defined by the reduction gear and motor nominal torque. So, the limit nominal torque for actuators 8, 10 and 11 is 70.4 N.m, as it is shown in the chart that each joint never overlap the nominal torque limit; it is notice that the knee joint have the highest torque, the gait pattern generated should have in account to reduce it.

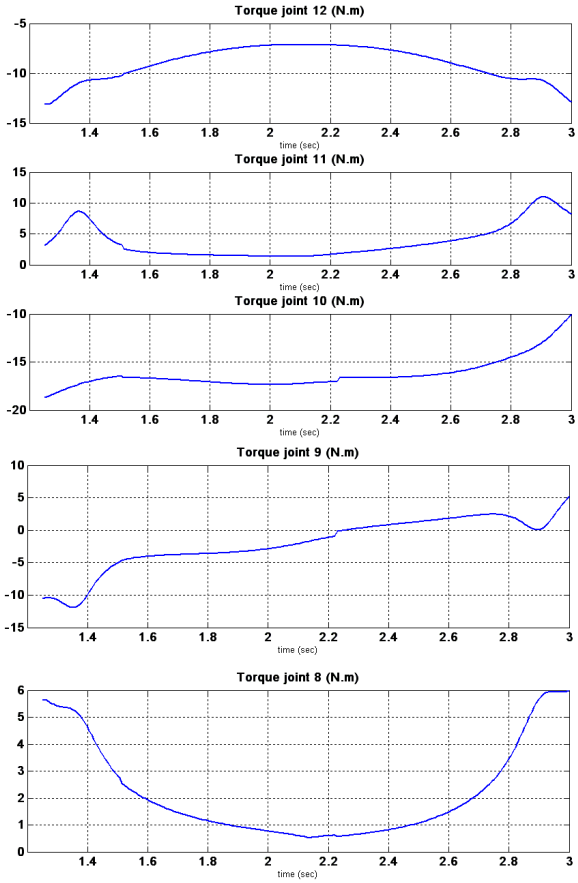

Fig. 5. Joints torque of the support foot in the *n-th* step.

The joint 9 torque limit is 44.8 Nm and the maximum torque obtained is 12 N.m, thus its acceptable. Finally, the 12 joint limit is 17.6 Nm, the chart shown 13 N.m as maximum, it is near the nominal one, because the frontal ankle joint has less reduction respect to other ones. Furthermore, this joint support overall humanoid robot mass during single support stage and it drives the frontal balance in order to maintain the ZMP inside the convex hull. We could conclude that the gait pattern generated have satisfied the nominal torque actuators limits, so it is validated, the gait pattern generation algorithm in this fact. The next section, other aspects as angular range and angular velocity constraints could be validated.

V. Simulation and Experimental Results

A. Rh-1 humanoid robot platform

Several simulation tests have been done in Rh-1 simulator software, developed under VRML environment, before to test in Rh-1 humanoid robot platform (Fig. 6), which specifications are described in Table I.

B. Gait patterns and kinematics constraints

Some gait patterns should be seen in Fig. 7, taking into account the angular joint range limits as see in Table I. The proposed gait generation algorithm allows to change

TABLE I

RH-1 HUMANOID ROBOT SPECIFICATIONS

Link	**Number of DOF**	**Total**
Head	-	-
Waist	1 (Yaw)	1
Arm	4	4x2
Shoulder	1 (Pitch) 1 (Roll)	
Elbow	1 (Pitch)	
Wrist	1 (Roll)	
Leg	6	6x2
Hip	1 (Yaw) 1 (Roll) 1 (Pitch)	
Knee	1 (Pitch)	
Ankle	1 (Pitch) 1 (Roll)	
	Total	***21***
Joint	**Human angular range (deg)**	**Rh-1 angular range (deg)**
Head	-50 to 50 (Roll) -50 to 60 (Pitch -70 to 70 (Yaw)	- - -
Arm		
Shoulder	-90 to 0 (Roll) -180 to 50 (Pitch) -90 to 90 (Yaw)	-95 to 0 (Roll) -180 to 60 (Pitch) -
Elbow	-145 to 90 (Pitch) -90 to 90 (Yaw)	-135 to 0 (Pitch) -
Wrist	-55 to 25 (Roll) -70 to 90 (Pitch)	-90 to 90 (Roll) -
Hand	0 to 90 (Pitch)	-16 to 60 (Pitch)
Waist	-50 to 50 (Roll) -30 to 45 (Pitch) -40 to 40 (Yaw)	- - -45 to 45 (Yaw)
Leg		
Hip	-45 to 20 (Roll) -125 to 15 (Pitch) -45 to 45 (Yaw)	-20 to 20 (Roll) -80 to 80 (Pitch) -15 to 15 (Yaw)
Knee	0 to 130 (Pitch)	0 to 100 (Pitch)
Ankle	-20 to 30 (Roll) -20 to 45 (Pitch)	-20 to 20 (Roll) -25 to 25 (Pitch)

direction while the humanoid is walking, continuous step length changing and walking in any surface. Angular velocity constraints have been satisfied as actuator limits, thus the smooth gait patterns could be validated; i.e the actuator knee angular velocity limit is 8000 RPM, the gait pattern generated is suitable for this requirement as we can see in Fig. 9.

C. VRML Rh-1 simulations

Snapshots for doing a circle and curve path on flat surface have shown in Fig. 8. Natural and smooth change direction could be done by the proposed algorithm, thus natural walking is obtained as human one. Furthermore, faster walking motion should be developed until 1 Km/h at any direction on flat surface; in another kind of surface slower walking motion by physical constraints and stability one would be obtained.

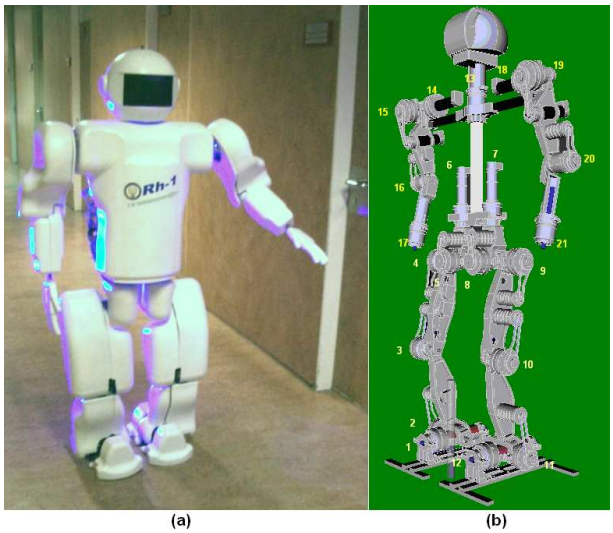

Fig. 6. Rh-1 humanoid robot (a) and its mechanical configuration (b).

D. Actual results on Rh-1 humanoid robot platform

In order to validate the proposed algorithm in the Rh-1 humanoid robot, many test have been done. As observed in Fig. 10, two examples of straight forward walking motion is shown, one in the lab (Fig. 10.a), and the other one in the hall (Fig. 10.b); experimental walking stable motion is obtained, so the algorithm is succesfully tested, up to 0.7 Km/h walking speed.

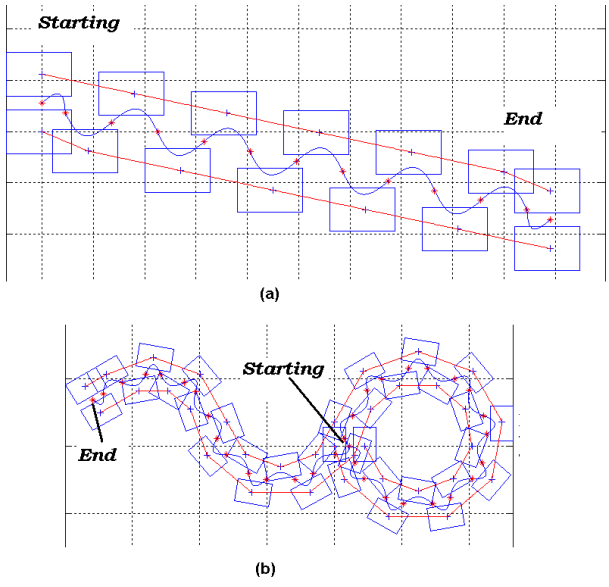

Fig. 7. Gait patterns generated for continuous humanoid walking. It is possible to generate diagonal walking (a), and any direction continuous walking (b).

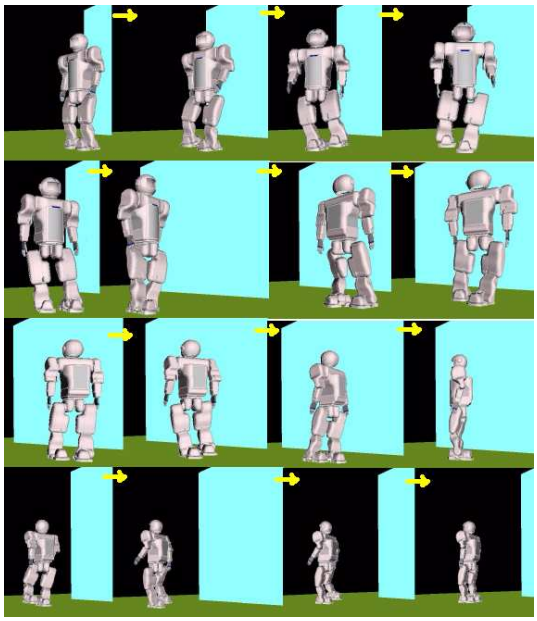

Fig. 8. Snapshots of VRML Rh-1 simulation, for smooth naturally and continuous walking as figure 7.b

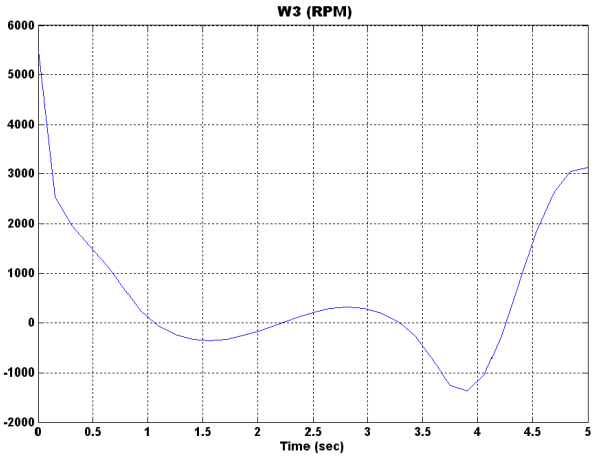

Fig. 9. The angular velocity requirement by knee joint, its actuator run up 8000 RPM.

VI. Conclusions

Foot and COG motion planning had been developed for applying in real time, by satisfying the stability criterion on bipedal walking robots, joint angle, angular velocity and torque conditions. Lagrange formulation, Lie groups and screw theory had been employed in order to verify the joint torques in the humanoid robot, while it is walking, thus dynamics constraints are obtained. Foot motion algorithm for any landing point had been developed and shown some simulations results. Simulation results on Rh-1 simulator environment had been shown, and it allows to test the gait patterns before to apply it in actual humanoid robot. The proposed algorithm has been tested in the actual Rh-1 humanoid robot, successfully.

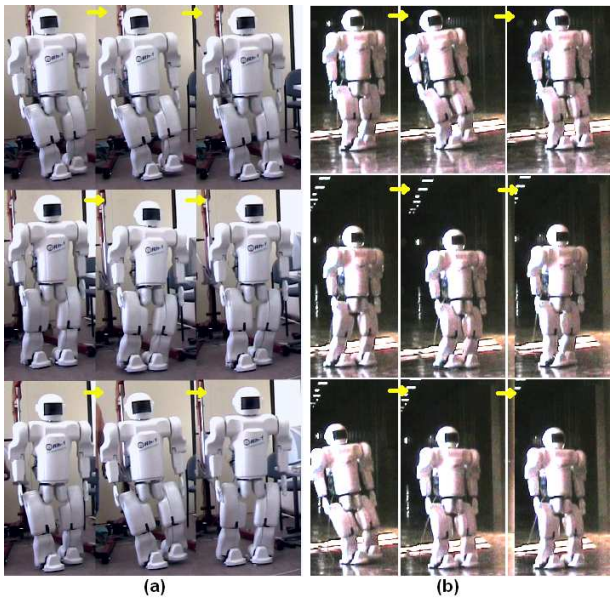

Fig. 10. Actual humanoid robot walking under LAG algorithm, (a) in the laboratory, (b) in the hall.

Currently works deal about global motion humanoid robot control, in order to improve its walking motion. The next step, is to make tests at uneven surfaces with an improved algorithm.

Acknowledgment

We would like to thank the members of the Robotics Lab of University Carlos III of Madrid for their cooperation an suggestions. We also express acknowledgment to the Humanoid team for their support. This research is supported by the CICYT (Comision Interministerial de Ciencia y Tecnologia), ref. DPI2004-00325.

References

[1] H. Lim, Y. Kanesima, and A. Takanishi, “Online walking pattern generation for biped humanoid robot with trunk,” in *Proceedings of the 2002 IEEE/RSJ Intl.Conference on Intelligent Robot and Systems*, 2002.

[2] M. Vukobratovic and A. Frank, “One the gait stability of biped machines,” *IEEE Transactions on Automatic Control*, 1970.

[3] S. Kajita, F. Kanehiro, K. Kaneko, K. Fujiwara, K. Harada, K. Yokoi, and H. Hirukawa, “Biped walking pattern generation by using preview control of zero-moment point,” in *IEEE International Conference on Robotics & Automation*, Taipei and Taiwan, September 14-19 2003, pp. 162–1626.

[4] S. Kajita, F. Kanehiro, K. Kaneko, K. Fujiwara, K. Yokoi, and H. Hirukawa, “Biped walking pattern generation by a simple 3d inverted pendulum model,” *Autonomous Robots*, vol. 17, 2003.

[5] M. Morisawa, K. Harada, S. Kajita, F. Kanehiro, K. Kaneko, K. Fujiwara, S. Nakaoka, and H. Hirukawa, “A biped pattern generation allowing immediate modifications of foot pacement in real-time,” in *Proceedings on Humanoids 2006*, 2006.

[6] Q. Huang, K. Yokoi, S. Kajita, K. Kaneko, H. Arai, N. Koyachi, and K. Tanie, “Planning walking patterns for a biped robot,” *IEEE Transactions on Robotics and Automation*, vol. 17, pp. 280–289, 2001.

[7] M. Arbulu, J. M. Pardos, L. Cabas, P. Staroverov, D. Kaynov, C. Perez, M. Rodriguez, and C. Balaguer, “Rh-0 humanoid full size robot’s control strategy based on the lie logic technique,” in *5th IEEE-RAS International Conference on Humanoid Robots*, Tsukuba, Japan, Dec. 4-6 2005, pp. 271–276.

[8] R. M. Murray, Z. Li, and S. S. Sastry, *Mathematical Introduction To Robotic Manipulation*, C. Press, Ed. CRC Press, 1994.